

## Phase diagrams of the $S = \frac{1}{2}$ quantum antiferromagnetic $XY$ model on the triangular lattice in magnetic fields

N. Suzuki and F. Matsubara

*Department of Applied Physics, Faculty of Engineering, Tohoku University, Sendai 980-77, Japan*

(Received 10 December 1996; revised manuscript received 29 January 1997)

We study the  $S = \frac{1}{2}$  quantum antiferromagnetic  $XY$  model on finite triangular lattices with  $N$  sites in both longitudinal and transverse magnetic fields. We calculate physical quantities in the ground state using a diagonalization for spins  $N \leq 27$ , and those at finite temperatures using a quantum transfer Monte Carlo method for  $N \leq 24$ . In the longitudinal magnetic field, the long-range chiral order parameter seems to have a finite, nonzero value at low temperatures suggesting the occurrence of a classical umbrella-type phase. In the transverse magnetic field, the  $1/3$  plateau of the magnetization curve appears even at low temperatures, in contrast with the classical model. The magnetic-field dependences of the order parameters suggest that the chiral-ordered, the ferrimagnetic, and the spin-flop phases appear successively as the magnetic field is increased. The transition temperatures are estimated from the peak position of the specific heat, and the phase diagrams are predicted in both longitudinal and transverse magnetic fields. [S0163-1829(97)02118-8]

### I. INTRODUCTION

The antiferromagnetic  $XY$  model on the triangular lattice has attracted much interest. The Hamiltonian is

$$\mathcal{H} = 2J \sum_{\langle i,j \rangle} (S_i^x S_j^x + S_i^y S_j^y) - H^\alpha \sum_i S_i^\alpha, \quad (1)$$

where  $J (>0)$  is the exchange integral,  $H^\alpha$  is an external magnetic field along the  $\alpha$  direction, and  $\langle i,j \rangle$  takes all the nearest-neighbor pairs. In the classical model, Miyashita and Shiba<sup>1</sup> found using the Monte Carlo method that a long-range chiral-ordered phase exists at low temperatures, although the long-range order of the spins disappears at finite temperatures. They also suggested that the transition belongs to the universality class of the Ising model. The model in magnetic fields was also studied. In a longitudinal field, all the spins lean to the  $z$  direction but the chiral-ordered phase still exists (Fig. 1, the umbrella-type phase). On the other hand, in a transverse magnetic field, Lee *et al.* showed that the chiral-ordered, the ferrimagnetic, and the spin-flop phases appear successively as the magnetic field increases [in Figs. 2(a)–2(c)].<sup>2</sup> In the ferrimagnetic phase, the magnetization has a value of  $\frac{1}{3}$  of the saturated value, and the magnetization curve exhibits a plateau, which is often called a  $\frac{1}{3}$  plateau. However, the ferrimagnetic region of the field shrinks as the temperature cools down, and vanishes at  $T=0$ .

In the  $S=1/2$  quantum model, it has been discussed whether the classical ordered phases are broken down by the quantum fluctuation or not.<sup>3–10</sup> The ground-state properties of the model on finite lattices have been studied using a diagonalization method.<sup>3–6</sup> The largest lattice treated up to now is that with  $N=36$ ,<sup>5</sup> and the results suggest that the chiral order parameter remains finite for  $N \rightarrow \infty$ . The properties at finite temperatures were also studied by several authors using a quantum transfer Monte Carlo (QTMC),<sup>7,11</sup> a high-temperature series expansion,<sup>8</sup> and a super-effective-field theory.<sup>9</sup> Recently, the authors carefully studied an an-

isotropic Heisenberg model using the QTMC method and showed that, when  $XY$  anisotropy is large, the peak height of the specific heat increases with  $N$ .<sup>12</sup> Thus they predicted that the quantum fluctuation does not destroy the classical chiral-ordered phase in finite temperatures. In the presence of magnetic fields, on the contrary, it was speculated that the quantum fluctuation brings a different ground state from the classical one. Chubukov and Golosov studied the ground state of the  $XY$  model in the transverse field using the spin-wave theory, and suggested that the  $1/3$  plateau appears at  $T=0$ .<sup>13</sup> However, the spin-wave theory does not always give a correct result in the frustrated model.<sup>14</sup> Moreover, when  $S=1/2$ , the critical field at which the plateau appears becomes negative because of the  $1/S$  expansion.<sup>13</sup>

In this paper, we study the  $S=1/2$  quantum  $XY$  model in magnetic fields. We consider the magnetic structures both at  $T=0$  and at  $T \neq 0$ . We calculate quantities in the ground state of finite lattices with  $N \leq 27$  by the diagonalization method. On the other hand, those in finite temperatures are calculated on the lattice with  $N \leq 24$  using the QTMC method. From the result, we suggest the following things. (1) In the longitudinal field, the umbrella-type phase occurs up to  $H^z = 3.0$ . (2) In the transverse field, the  $1/3$  plateau really appears even in the ground state. The chiral-ordered, the fer-

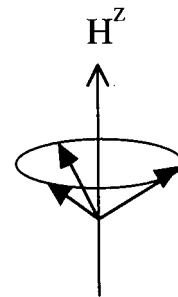


FIG. 1. A spin structure of the classical model in the longitudinal magnetic field, which is called the umbrella-type phase.

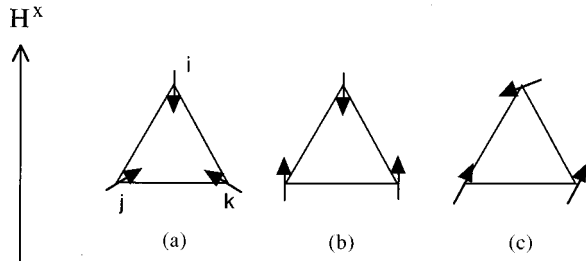


FIG. 2. Three spin structures of the classical model in the transverse magnetic field. (a) The chiral-ordered phase, (b) the ferrimagnetic phase, and (c) the spin-flop phase.

rimagnetic, and the spin-flop phases occur as the magnetic field is increased. The phase diagrams in both longitudinal and transverse fields are predicted.

We consider the models in the longitudinal and the transverse fields in Secs. II and III, respectively. The summary is given in Sec. IV. We explain the QTMC method in the Appendix.

## II. LONGITUDINAL MAGNETIC FIELD

In this section, we study the model in a longitudinal field  $H^z$ . First, we consider the magnetization and the chiral order parameter in the ground state. The total magnetization along the external field  $H^z$  is given by

$$M^z = (1/N) \sum_i S_i^z. \quad (2)$$

The  $z$  component of the chirality of the upright triangle at  $\mathbf{R}$  is defined as

$$\chi^z(\mathbf{R}) = \frac{1}{\sqrt{3}} (S_i^x S_j^y - S_i^y S_j^x + S_j^x S_k^y - S_j^y S_k^x + S_k^x S_i^y - S_k^y S_i^x), \quad (3)$$

where the relation of  $i \rightarrow j \rightarrow k$  is taken counterclockwise, as is shown in Fig. 2(a). The eigenvalues of  $\chi^z(\mathbf{R})$  are  $\pm 1/2$  and 0. The long-range chiral order parameter is defined as

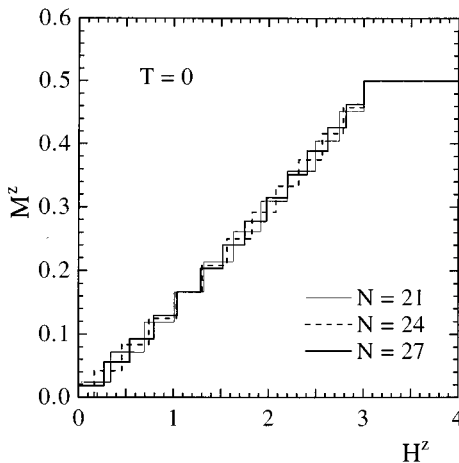


FIG. 3. The field dependence of the magnetization  $M^z$  at  $T=0$ .

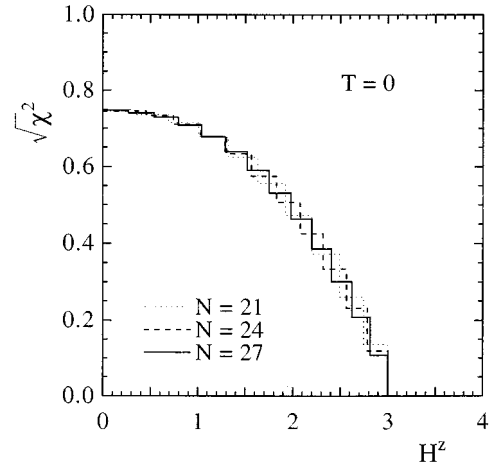


FIG. 4. The field dependence of the chiral order parameter  $\sqrt{\chi^2}$  at  $T=0$ .

$$\chi^2 = \frac{1}{NS(NS+1)} \left[ \sum_{\mathbf{R} \in \Delta} \chi^z(\mathbf{R}) \right]^2, \quad (4)$$

where  $\mathbf{R}$  runs over all the upright triangles on the lattice. In Figs. 3 and 4, we show  $M^z$  and  $\sqrt{\chi^2}$ , respectively. Since their size dependences are almost negligible, these values will be similar to those for  $N \rightarrow \infty$ . The magnetization increases almost linearly with  $H^z$ , and no anomaly is observed until the saturated field  $H_{\max}^z = 3.0$ . The chiral order parameter decreases monotonically with increasing  $H^z$ , and vanishes at  $H_{\max}^z = 3.0$ . These results suggest that the chiral-ordered phase changes into an umbrella-type one, and it survives up to  $H_{\max}^z = 3.0$ . If it is true, the chiral order parameter at  $H^z \neq 0$  will be approximately given as  $\sqrt{\chi^2} = \sqrt{\chi^2}_{H^z=0} \cos^2 \theta = \sqrt{\chi^2}_{H^z=0} [1 - (M^z)^2]$ , where  $\theta$  is the angle between the spin and  $XY$  plane. We calculate  $\sqrt{\chi^2}$  and show it in Fig. 5 together with  $\sqrt{\chi^2}$ . The two results are in good agreement with each other. Thus we may conclude that in the ground state the umbrella-type phase occurs at  $H^z \neq 0$ , and it survives up to  $H_{\max}^z = 3.0$ .

Next we consider  $\langle M^z \rangle$  and  $\sqrt{\langle \chi^2 \rangle}$  for a finite temperature, where  $\langle \dots \rangle$  denotes the thermal average. All the results

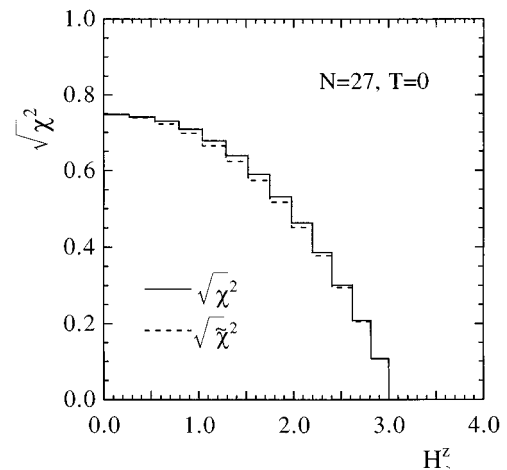


FIG. 5.  $\sqrt{\chi^2}$  and  $\sqrt{\chi^2}$  at  $T=0$ .

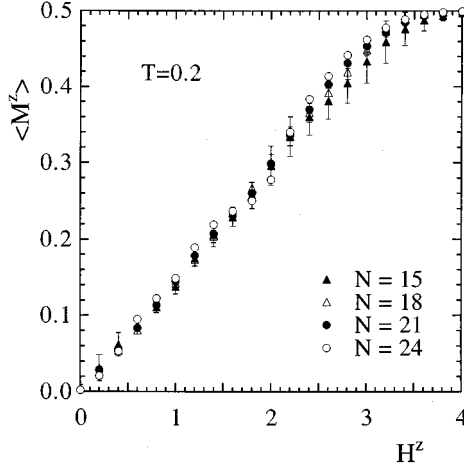


FIG. 6. The field dependence of  $\langle M^z \rangle$  at  $T=0.2$ .

presented below have been obtained by the QTM method (see the Appendix). The number of the states  $M$  used in the QTM calculation are as follows:  $M=50$  for  $N=9-18$ ,  $M=10$  for  $N=21$ , and  $M=2$  for  $N=24$ . For every lattice except for  $N=24$ , the set of  $M$  states is divided into five subsets, and quantities of interest are calculated in every subset. Error bars presented in figures given below only mean deviations of the values obtained in different subsets. In the QTM calculation, since the operators  $\mathcal{H}_0 = 2J\Sigma(S_i^x S_j^x + S_i^y S_j^y)$  and  $\mathcal{H}_1 = -H^z \Sigma S_i^z$  are commutable,  $\exp[-(\mathcal{H}_0 + \mathcal{H}_1)/T]$  may be decomposed into  $\exp[-\mathcal{H}_0/T] \exp[-\mathcal{H}_1/T]$ . Therefore, we can calculate the quantities for a finite temperature combining the  $T$  transfer and the  $H^z$  transfer. That is, those quantities are transferred from a high temperature,  $T_0$ , to a temperature of interest,  $T_{\text{fin}}$ , by operating  $\exp[-\mathcal{H}_0/T_0]$ . Then, the field is increased by the operator  $\exp[-\mathcal{H}_1/T_{\text{fin}}]$ . In Figs. 6 and 7, we show  $\langle M^z \rangle$  and  $\sqrt{\langle \chi^2 \rangle}$  at  $T=0.2$  for different  $N$ , respectively. In low fields, the results are very similar to those of the ground state and their size dependences are small. As  $H^z$  is increased beyond  $H^z=2.5$ , their size dependences become considerable. Therefore, we suggest that at  $T=0.2$  the umbrella-type phase survives at least  $H^z \lesssim 2.5$ .

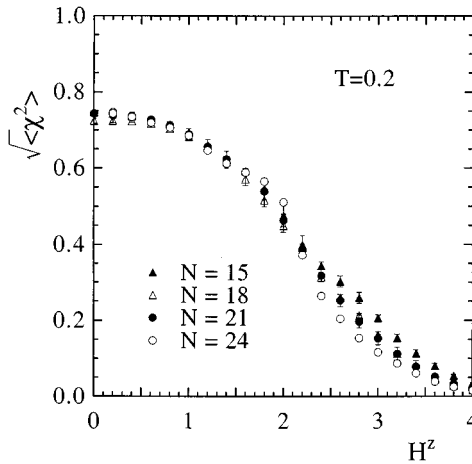


FIG. 7. The field dependence of  $\sqrt{\langle \chi^2 \rangle}$  at  $T=0.2$ .

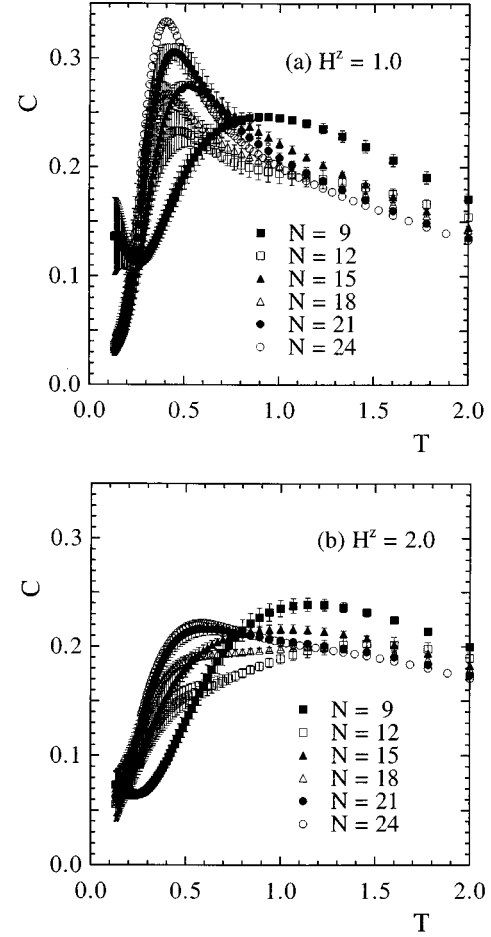


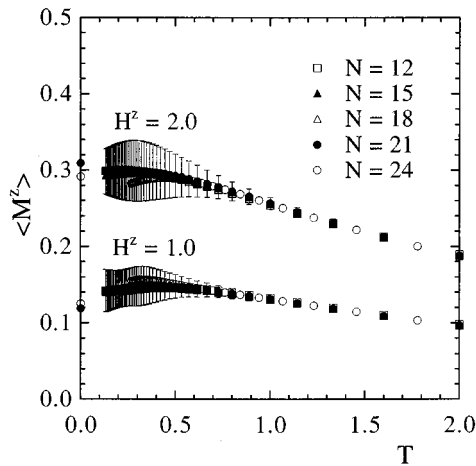
FIG. 8. The temperature dependence of the specific heat  $C$  for different  $H^z$ : (a)  $H^z=1.0$  and (b)  $H^z=2.0$ .

We also consider the temperature dependence of the specific heat  $C$ ,  $\langle M^z \rangle$ , and  $\sqrt{\langle \chi^2 \rangle}$  at fixed fields. The specific heat is calculated from

$$C = \frac{1}{T^2} (\langle \mathcal{H}^2 \rangle - \langle \mathcal{H} \rangle^2). \quad (5)$$

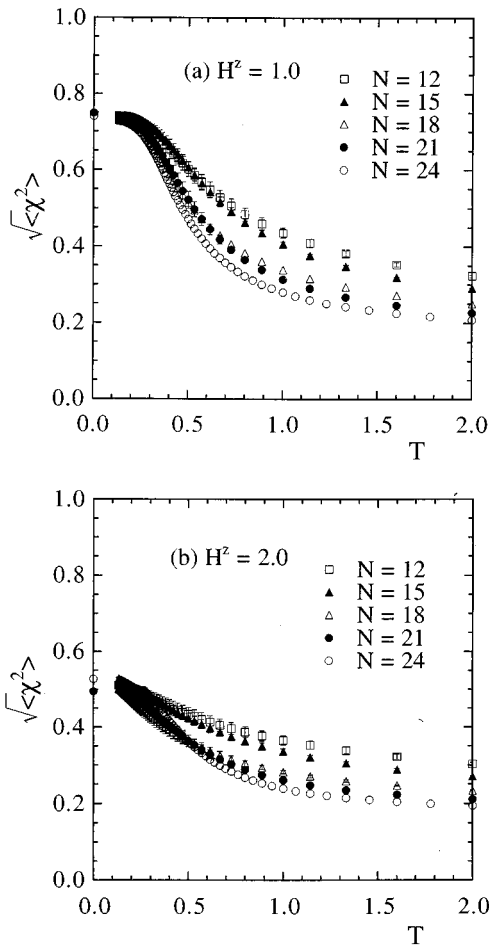
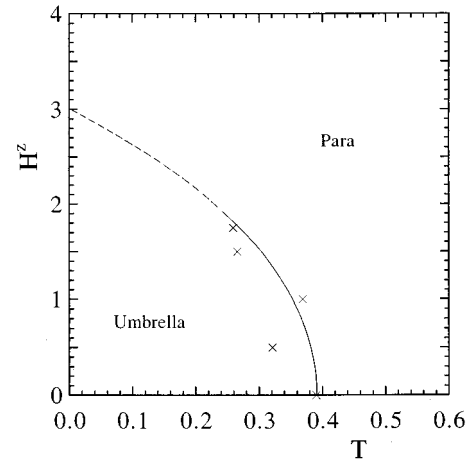
We found considerable differences in those quantities between for odd  $N$  and for even  $N$ , but they are reduced with increasing  $N$ . In Fig. 8(a), we plot  $C$  as a function of  $T$  at  $H^z=1.0$ . As  $N$  increases, the peak of  $C$  becomes higher and sharper at  $T \sim 0.4$ . A similar size dependence can be seen up to  $H^z \sim 2.0$ . Results at  $H^z=2.0$  are also shown in Fig. 8(b), in which the increase of  $C$  is seen at low temperatures. In Figs. 9 and 10, we plot  $\langle M^z \rangle$  and  $\sqrt{\langle \chi^2 \rangle}$  as functions of  $T$ . As the temperature is lowered,  $\langle M^z \rangle$  increases slowly and saturates at  $T \sim 0.4$ .  $\sqrt{\langle \chi^2 \rangle}$  increases and its size dependence becomes smaller, which indicates that  $\sqrt{\langle \chi^2 \rangle}$  remains finite in the thermodynamic limit. Therefore all the results suggest that the phase transition occurs at least  $H^z \leq 2.0$ .

The phase diagram of the model predicted from the above results is shown in Fig. 11. The transition line is estimated from the peak position of  $C$ . The chiral-ordered phase with the longitudinal magnetization (the umbrella-type phase) survives in the longitudinal magnetic field  $H^z$ .

FIG. 9. The temperature dependence of  $\langle M^z \rangle$ .

### III. TRANSVERSE MAGNETIC FIELD

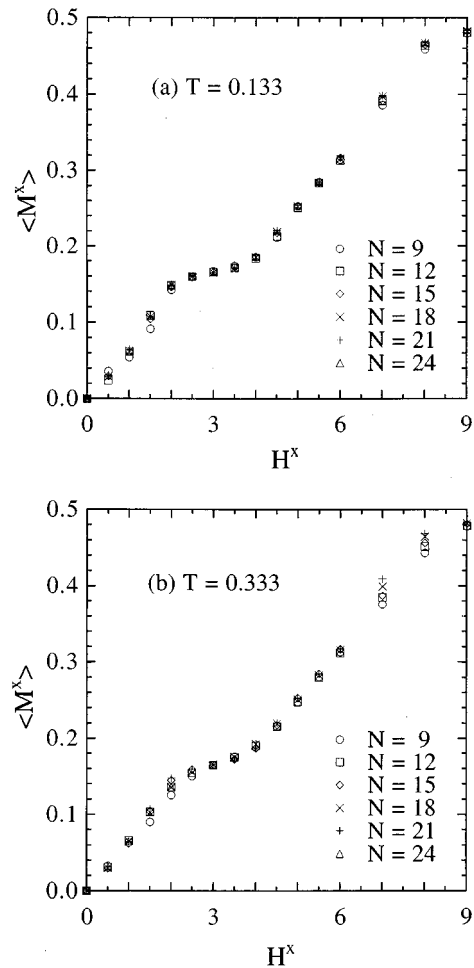
Next we study the model in the transverse field  $H^x$ . Since the total magnetization  $M^z$  is not good quantum number, we must treat all the  $2^N$  states in the diagonalization method. The QTM method prepares all the Ising states, and it does not suffer from this difficulty. We calculate the magnetization, the order parameter defined below, and the specific

FIG. 10. The temperature dependence of  $\sqrt{\langle \chi^2 \rangle}$  for different  $H^z$ : (a)  $H^z = 1.0$  and (b)  $H^z = 2.0$ .FIG. 11. Phase diagram in longitudinal fields. The symbol  $\times$  is estimated from the peak position of the specific heat. The line is a guide to the eye.

heat. The number of the states  $M$  are as follows:  $M = 50$  for  $N \leq 18$ ,  $M = 10$  for  $N = 21$ , and  $M = 2$  for  $N = 24$ .

We calculate the total magnetization given by

$$M^x = \sum_i S_i^x / N. \quad (6)$$

FIG. 12. The field dependence of the magnetization  $\langle M^x \rangle$  for different  $T$ : (a)  $T = 0.133$  and (b)  $T = 0.333$ .

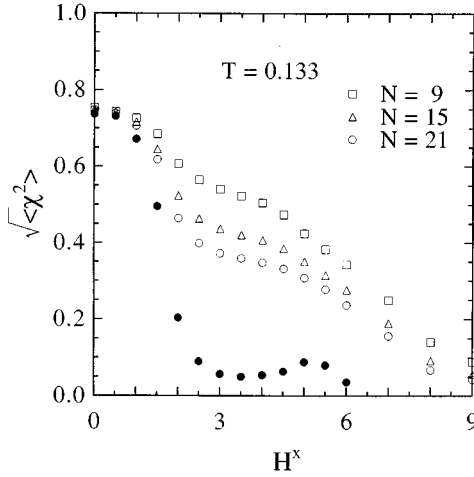


FIG. 13. The chiral order parameter  $\sqrt{\langle \chi^2 \rangle}$  vs  $H^x$ . The symbol  $\bullet$  denotes the extrapolated value.

This quantity becomes 1/6 if the ferrimagnetic phase appears and 1/2 if all the spins align along the  $x$  direction. In Figs. 12(a) and 12(b), we show the magnetization as functions of  $H^x$  at  $T=0.133$  and  $0.333$ , respectively. The data for different  $N$  lie almost on the same line, and the temperature dependence is negligibly small. Note that we also calculate  $\langle M^x \rangle$  in the ground state for  $N=12$ , and find the result is quite similar to that at  $T=0.133$ . There is the 1/3 plateau in the region of  $2.0 \leq H^x \leq 4.0$ . We estimate two edges of the plateau  $H_{c1}$  and  $H_{c2}$  at various temperatures, and plot them in the phase diagram shown below. These edges depend little on the temperature. Note that even at  $T=0.133$ ,  $\langle M^x \rangle$  slightly increases with  $H^x$  between  $H_{c1}$  and  $H_{c2}$ , in contrast with that of the Heisenberg model,<sup>13,15</sup> because  $\langle M^x \rangle$  is not good quantum number in the  $XY$  model.

Now we consider the spin structure. In Fig. 2, we show three possible spin structures (a), (b), and (c) which appear in the classical model at low, intermediate, and high fields, respectively. These structures are called as the chiral-ordered, the ferrimagnetic, and the spin-flop phases, respectively. In order to see which structure is realized with  $H^x$ , we calculate the chiral order parameter and  $x$  and  $y$  components of the sublattice order parameters which are defined as

$$\mathcal{M}^\alpha = \left[ \frac{1}{2} \langle (M_A^\alpha - M_B^\alpha)^2 + (M_B^\alpha - M_C^\alpha)^2 + (M_C^\alpha - M_A^\alpha)^2 \rangle \right]^{1/2}, \quad (7)$$

where  $M_\zeta^\alpha [\equiv \sum_{i \in \zeta} S_i^\alpha / (N/3)]$  means the  $\alpha$  component of the magnetization of the  $\zeta$  sublattice. In Table I we show the relation between the order parameters and the spin structures. In Figs. 13–15, we plot  $\sqrt{\langle \chi^2 \rangle}$ ,  $\mathcal{M}^x$ , and  $\mathcal{M}^y$ , respectively,

TABLE I. The relation between the order parameters and the classical spin structures.

	Structure (a)	Structure (b)	Structure (c)
$\sqrt{\langle \chi^2 \rangle}$	$\neq 0$	$= 0$	$= 0$
$\mathcal{M}^x$	$\neq 0$	$\neq 0$	$\neq 0$
$\mathcal{M}^y$	$\neq 0$	$= 0$	$\neq 0$

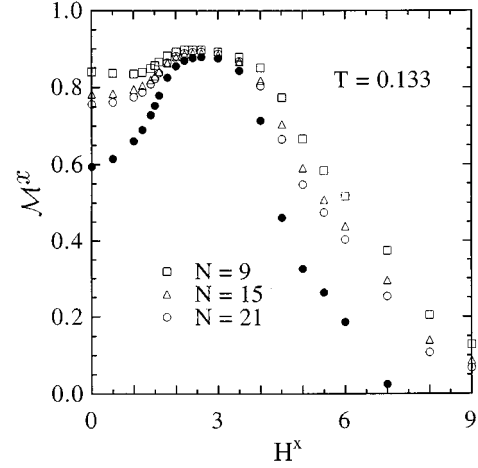


FIG. 14. The order parameter  $\mathcal{M}^x$  vs  $H^x$ . The symbol  $\bullet$  denotes the extrapolated value.

as functions of  $H^x$  at  $T=0.133$ . When  $H^x < H_{c1}$ , their size dependences are not so large. Especially, for  $H^x \leq 1.0$ ,  $\sqrt{\langle \chi^2 \rangle}$  depends very little on  $H^x$ . As  $H^x$  reaches  $H_{c1}$ ,  $\sqrt{\langle \chi^2 \rangle}$  and  $\mathcal{M}^y$  decrease markedly and their size dependences become larger. On the contrary,  $\mathcal{M}^x$  increases and its size dependence becomes small. When  $H_{c1} < H^x < H_{c2}$ ,  $\sqrt{\langle \chi^2 \rangle}$  and  $\mathcal{M}^y$  remarkably depend on the system sizes. On the other hand, the size dependence of  $\mathcal{M}^x$  is negligible. When  $H^x > H_{c2}$ ,  $\mathcal{M}^x$  decreases and its size dependence is considerable.  $\mathcal{M}^y$  increases again and its size dependence is smaller, but  $\sqrt{\langle \chi^2 \rangle}$  still decreases. We tentatively assume that the data fit on the  $1/\sqrt{N}$  function, and estimated the values for  $N \rightarrow \infty$  which are also shown in the figures. When  $H^x < H_{c1}$ ,  $\sqrt{\langle \chi^2 \rangle}$ ,  $\mathcal{M}^x$ , and  $\mathcal{M}^y$  have a finite, nonzero value. When  $H_{c1} < H^x < H_{c2}$ ,  $\sqrt{\langle \chi^2 \rangle}$ , and  $\mathcal{M}^y$  seem to vanish for  $N \rightarrow \infty$ , whereas  $\mathcal{M}^x$  remains finite. When  $H_{c2} \leq H^x$ ,  $\mathcal{M}^x$  and  $\mathcal{M}^y$  have a finite, nonzero values, but  $\sqrt{\langle \chi^2 \rangle}$  disappears. From these results, we suggest that the structures (a), (b), and (c) in Fig. 2 occur when  $H^x < H_{c1}$ ,  $H_{c1} < H^x < H_{c2}$ , and  $H_{c2} < H^x$ , respectively. Of course, these picture of the spin structure are compatible with the magnetization curve which are shown in Figs. 12.

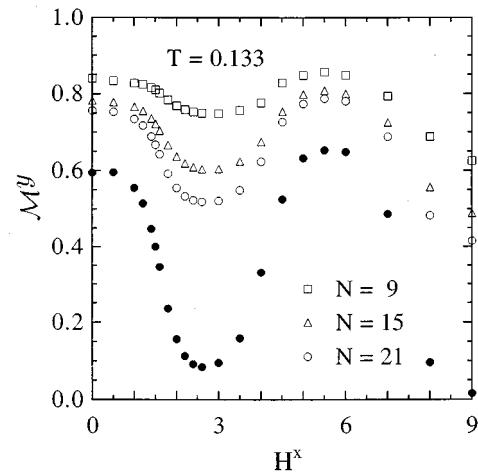


FIG. 15. The order parameter  $\mathcal{M}^y$  vs  $H^x$ . The symbol  $\bullet$  denotes the extrapolated value.

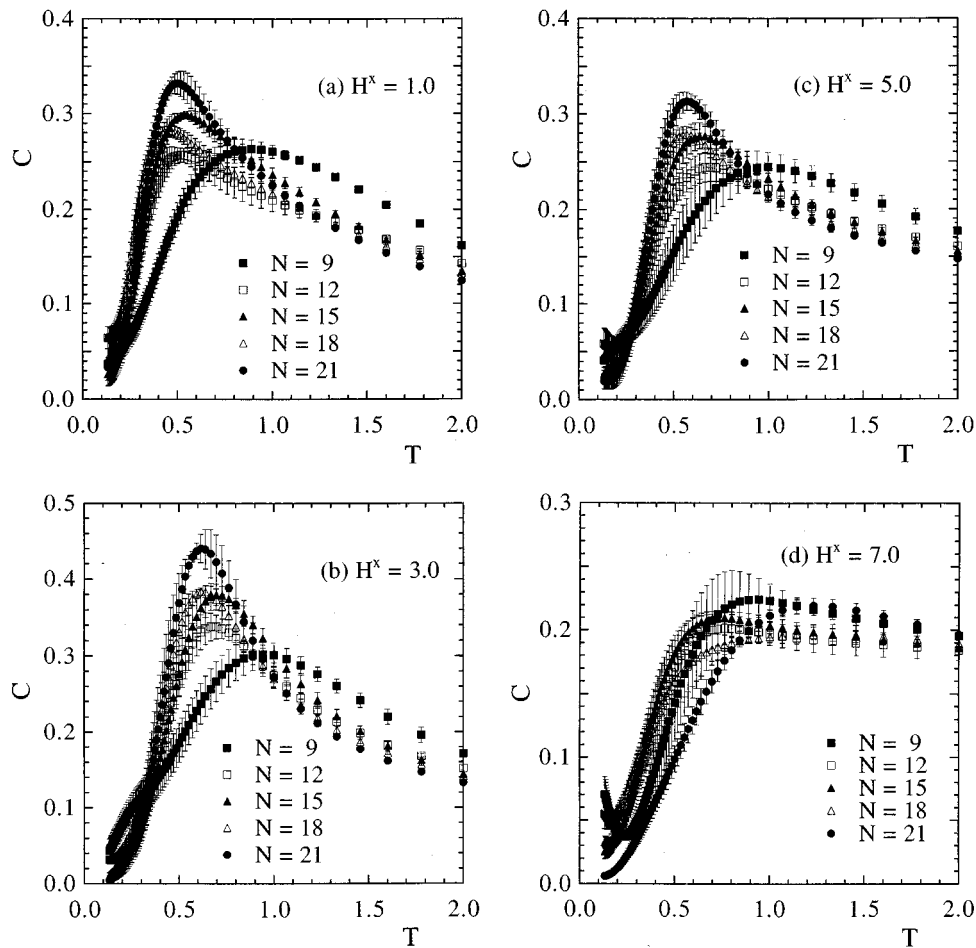


FIG. 16. The temperature dependence of the specific heat  $C$  for different  $H^x$ : (a)  $H^x=1.0$ , (b)  $H^x=3.0$ , (c)  $H^x=5.0$ , and (d)  $H^x=7.0$ .

In Figs. 16(a)–16(d), we present the specific heat  $C$  at  $H^x=1.0, 3.0, 5.0$ , and  $7.0$ . For  $H^x \leq 5.0$ , the peak height becomes higher with increasing  $N$  suggesting the occurrence of the phase transition. At  $H^x=7.0$ , the peak height does not increase with  $N$ , but  $C$  does at low temperatures. Therefore we expect that the phase transition also takes place at  $H^x=7.0$ . The transition temperatures are estimated from the size dependence of the peak temperature  $T_m$ .<sup>12</sup>

In Fig. 17, we show the phase diagram of the model. This phase diagram is analogous to that of the classical model. However, it should be emphasized that the  $1/3$  plateau widely survives at the low temperatures.

#### IV. SUMMARY

In this paper, we have studied the  $S=1/2$  quantum anti-ferromagnetic  $XY$  model on finite triangular lattice in both longitudinal and transverse magnetic fields using the diagonalization and the QTM methods. We have calculated the magnetization, the specific heat, and the order parameters for different sizes of the lattices, and examined their size dependences to see whether some long-range ordered phase occurs or not. Our results are summarized as follows.

In the longitudinal magnetic field, the long-range chiral order parameter seems to have a finite, nonzero value at low temperatures. The peak height of the specific heat increases with  $N$  suggesting the occurrence of the phase transition.

From the results, we suggest that the umbrella-type phase survives at low temperatures, and predict the phase diagram.

In the transverse magnetic field, the  $1/3$  plateau is seen in the magnetization curve at low temperatures, in contrast with the classical model. The behavior of the order parameters

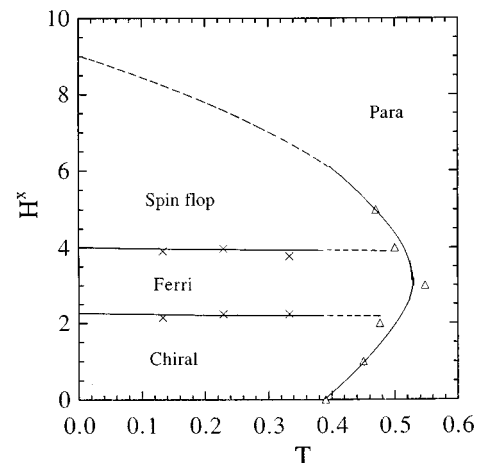


FIG. 17. Phase diagram in transverse fields. The symbols  $\times$  and  $\triangle$  are estimated from the edges of the plateau of the magnetization curve and the peak height of the specific heat, respectively. The lines are guides to the eye.

suggests that the chiral-ordered, the ferrimagnetic, and the spin-flop phases appear successively as the field is increased. The peak height of the specific heat increases with  $N$  suggesting the occurrence of the long-range order. Thus we suggest that the three phases occur in the transverse magnetic field at finite temperatures as in the classical model. The quantum fluctuation destroys the order of the  $y$  component of the spin, and the ferrimagnetic phase appears at low temperatures.

We would like to thank Dr. T. Nakamura for valuable discussions. The diagonalization programs are based on the subroutine package ‘‘TITPACK Ver. 2’’ coded and supported by Professor H. Nishimori, and ‘‘KOBEPACK/S Ver. 1.1’’ by Professor T. Tonegawa, Professor M. Kaburagi, and Dr. T. Nishino. The computation in this work has been done using the facilities of the Supercomputer Center, Institute for Solid State Physics, University of Tokyo. This work was supported by Grant-in-Aid for Scientific Research from the Ministry of Education, Science, and Culture.

#### APPENDIX: THE QTMC METHOD

In QTMC method,<sup>11,12</sup> we calculate the following quantity:

$$\langle \widehat{A} \rangle = \frac{\sum_k^M \langle \psi_k | A \exp(-\beta H) | \psi_k \rangle}{\sum_k^M \langle \psi_k | \exp(-\beta H) | \psi_k \rangle}, \quad (\text{A1})$$

where  $A$  is some physical operator and the sum runs over  $M$  states each of which is given by

$$|\psi_k\rangle = \sqrt{\frac{6}{M}} \sum_i^{2^N} C_{ik} |i\rangle, \quad (\text{A2})$$

here  $C_{ik}$  is a random number of  $-1 \leq C_{ik} \leq 1$ . We can readily show that  $\langle \widehat{A} \rangle \rightarrow \langle A \rangle$  for  $M \rightarrow \infty$ , because  $(6/M) \sum_k^M C_{ik} C_{jk} = \delta_{ij} + O(1/\sqrt{M})$ .<sup>12</sup> A great advantage of using formula (A1) is that we can obtain an approximate value of the average  $\langle A \rangle$  by summing up only  $M$  terms instead of all the  $2^N$  terms of the Ising states. Using this formula, we can treat systems much larger than those treatable by the rigorous formula. Of course, statistical errors of  $O(1/\sqrt{M})$  arise, but we may reduce them as  $M$  is increased.

- 
- <sup>1</sup>S. Miyashita and H. Shiba, J. Phys. Soc. Jpn. **53**, 1145 (1984); S. Miyashita, Prog. Theor. Phys. Suppl. No. 87, 112 (1986).  
<sup>2</sup>D. H. Lee, J. D. Joannopoulos, J. W. Negele, and D. P. Landau, Phys. Rev. B **33**, 450 (1986).  
<sup>3</sup>S. Fujiki and D. D. Betts, Can. J. Phys. **65**, 76 (1987); Prog. Theor. Phys. Suppl. No. 87, 268 (1986).  
<sup>4</sup>H. Nishimori and H. Nakanishi, J. Phys. Soc. Jpn. **57**, 626 (1988).  
<sup>5</sup>P. W. Leung and K. J. Runge, Phys. Rev. B **47**, 5861 (1993).  
<sup>6</sup>N. Suzuki and F. Matsubara, J. Phys. Soc. Jpn. **65**, 1121 (1996).  
<sup>7</sup>F. Matsubara and S. Inawashiro, Solid State Commun. **67**, 229

- (1988).  
<sup>8</sup>S. Fujiki and D. D. Betts, J. Phys. Soc. Jpn. **60**, 435 (1991).  
<sup>9</sup>T. Momoi and M. Suzuki, J. Phys. Soc. Jpn. **61**, 3277 (1992).  
<sup>10</sup>T. Momoi and M. Suzuki, J. Phys. Soc. Jpn. **61**, 3732 (1992).  
<sup>11</sup>M. Imada and M. Takahashi, J. Phys. Soc. Jpn. **55**, 3354 (1986).  
<sup>12</sup>N. Suzuki and F. Matsubara, Phys. Rev. B **51**, 6402 (1995).  
<sup>13</sup>A. V. Chubukov and D. I. Golosov, J. Phys. C **3**, 69 (1991).  
<sup>14</sup>P. Chandra and B. Doucot, Phys. Rev. B **38**, 9335 (1988).  
<sup>15</sup>H. Nishimori and S. Miyashita, J. Phys. Soc. Jpn. **55**, 4450 (1986).